crystals

MDPI

Article

Pseudo-Bifurcated Chalcogen Bond in Crystal Engineering

Yu Zhang and Weizhou Wang *

College of Chemistry and Chemical Engineering, and Henan Key Laboratory of Function-Oriented Porous Materials, Luoyang Normal University, Luoyang 471934, China; yzhpaper@yahoo.com

* Correspondence: wzw@lynu.edu.cn; Tel.: +86-379-6861-8320

Received: 2 March 2018; Accepted: 6 April 2018; Published: 9 April 2018

Abstract: The concept of pseudo-bifurcated chalcogen bond has been proposed for the first time in this paper. It was found that the anticooperative effects between two chalcogen bonds of the pseudo-bifurcated chalcogen bond are not very large as compared to those of the true bifurcated noncovalent bond. According to the nature of pseudo-bifurcated chalcogen bond, we designed some strong pseudo-bifurcated chalcogen bond synthons. The binding energy of the strongest pseudo-bifurcated chalcogen bond attains about 27 kcal/mol. These strong pseudo-bifurcated chalcogen bond synthons have great potential as building blocks in crystal engineering.

Keywords: chalcogen bond; bifurcated chalcogen bond; pseudo-bifurcated chalcogen bond; synthons; crystal engineering

1. Introduction

The effectiveness of the halogen bond in crystal engineering has been widely documented over the past decade [1–12]. In contrast, the study of the chalcogen bond, another type of noncovalent bond in which chalcogen acts as an electron acceptor, is still in its infancy, and many more studies must be carried out to understand the value of the chalcogen bond in crystal engineering [13–38]. Both the halogen bond and the chalcogen bond are of the σ-hole bond [39–42]. It is the regions of positive electrostatic potential on the outer surfaces of halogens and chalcogens that lead to the formation of the halogen bond and chalcogen bond (Figure 1). The structures and properties of the halogen bond and chalcogen bond are very similar. For example, in most cases, both are highly directional, electrostatically-driven noncovalent interactions [41,42]. However, as shown in Figure 1, halogens have only one electrophilic end whereas chalcogens always have two electrophilic ends, which causes that the structures and properties of the chalcogen bond may also be different from the ones of the halogen bond. At least, it is natural to suppose that the formation of the bifurcated chalcogen bond is much easier than the formation of the bifurcated halogen bond.

To better understand the difference between the halogen bond and the chalcogen bond, we carried out a statistical analysis of the iodine bonds and selenium bonds with nitrogen acceptors using the Cambridge Structural Database (CSD, version 5.27, November 2006 plus 31 updates, ConQuest version 1.8) [43,44]. The iodine bond is a subset of the halogen bond and the selenium bond is a subset of the chalcogen bond [7]. For simplicity, we did not consider the other subsets of the halogen bond and chalcogen bond. For the CSD search, only structures with not disordered, no errors, not polymeric, and no ions were considered. At the same time, the following general search filters were also chosen from the ConQuest search menu: 3D coordinates determined, only organics, and *R* factor < 0.05. It can be clearly seen from Scheme 1 that the CSD search yields 465 individual crystal structures containing the iodine bonds and 120 individual crystal structures containing the selenium bonds. Among each kind of crystal structures, the percentage of the crystal structures containing the bifurcated iodine

bonds and bifurcated selenium bonds are 3% (16 hits) and 22% (26 hits), respectively. This result supports the above hypothesis that the formation of the bifurcated chalcogen bond is much easier than the formation of the bifurcated halogen bond.

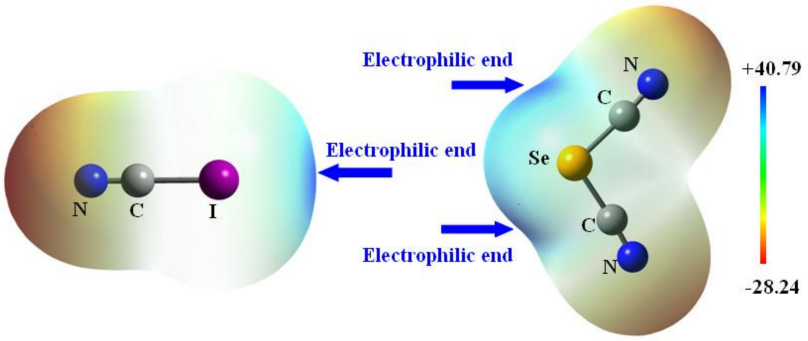

Figure 1. The electrostatic potentials on the 0.0004 au isodensity surfaces of NCI and $(NC)_2Se$ with a scale of −28.24 to +40.79 kcal/mol.

Scheme 1

I•••N
465 hits
Iodine bonds

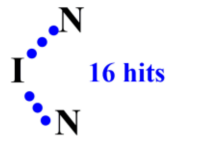

16 hits
Bifurcated iodine bonds

Se•••N
120 hits
Selenium bonds

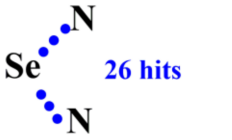

26 hits
Bifurcated selenium bonds

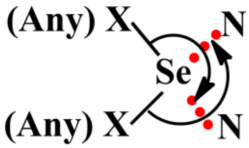

∠ X–Se•••Y (150°to 180°): 6 hits
Pseudo-bifurcated selenium bonds

Scheme 1. A CSD search of the noncovalent bonds considered.

Of the 26 bifurcated selenium bonds in Scheme 1, 6 fall between 150° and 180° for ∠X−Se···Y. Considering that the selenium atoms have two electrophilic regions and a noncovalent bond is always defined as a net attractive interaction between an electrophilic region and a nucleophilic region [6], the 6 bifurcated selenium bonds actually are not true bifurcated selenium bonds. Evidently, each of them also cannot be regarded as a simple combination of two separate selenium bonds. Consequently, the term "pseudo-bifurcated" selenium bond should be a more accurate descriptor of this kind of noncovalent bonds. Similarly, the pseudo-bifurcated selenium bond is also a subset of the pseudo-bifurcated chalcogen bond. We did not find the pseudo-bifurcated chalcogen bonds with two bond angles less than 150° in the CSD. Hence, the pseudo-bifurcated chalcogen bond can be defined as the bifurcated chalcogen bond which has two bond angles in the range of 150–180°.

The aim of this paper is two-fold. First, we will compare the difference between the pseudo-bifurcated noncovalent bonds and the true bifurcated noncovalent bonds. Second, according

to the nature of the pseudo-bifurcated chalcogen bond, we will design some strong pseudo-bifurcated chalcogen bond synthons which may have great potential in crystal engineering.

2. Computational Details

In the present study, selecting selenium dicyanide [$(NC)_2Se$], sulfur dicyanide [$(NC)_2S$], tellurium dicyanide [$(NC)_2Te$] and iodine cyanide (NCI) as chalcogen (halogen) atom donors and hydrogen cyanide (HCN), 1,10-phenanthroline (Phen) and *N*,*N*,*N*′,*N*′-tetramethyl-ethane-1,2-diamine (TMEDA) as chalcogen (halogen) atom acceptors, we studied the structures, energies and properties of the complexes formed by these chalcogen (halogen) atom donors with these chalcogen (halogen) atom acceptors. For all the model complexes considered in this paper, the geometries were fully optimized, and the binding energies were calculated at the B3LYP-D3/def2-TZVPP level of theory [45,46]. Here, B3LYP-D3 is the standard B3LYP method which is added by the D3 version of Grimme's dispersion with Becke-Johnson damping [47]. The reliability of the B3LYP-D3 method for the study of the noncovalent complexes can be found elsewhere [45]. It is well known that the accuracy of density functional theory calculations also depends on the number of points used in the numerical integration. An "ultrafine" integration grid (99 radial, 590 angular points) is used for all the density functional theory calculations to avoid the possible integration grid errors. The binding energies were calculated with the supermolecule method and corrected for basis set superposition error using the counterpoise method of Boys and Bernardi [48]. All the calculations were carried out with the GAUSSIAN 09 electronic structure program package [49].

Bader's "atoms in molecules" (AIM) theory, which is based on a topological analysis of the electron charge density and its Laplacian, has been widely applied in the study of the noncovalent bonds [50–52]. In this study, AIM analysis was also performed with the AIM2000 software package using B3LYP-D3/def2-TZVPP wave functions as input [53].

3. Results and Discussion

What is the difference between the pseudo-bifurcated noncovalent bonds and the true bifurcated noncovalent bonds? To answer this question, we selected the complexes NCI···NCH, NCI···$(NCH)_2$, $(NC)_2Se$···NCH and $(NC)_2Se$···$(NCH)_2$ as models to calculate their geometries and energies. NCI···$(NCH)_2$ contains the true bifurcated iodine bond and $(NC)_2Se$···$(NCH)_2$ contains the pseudo-bifurcated selenium bond. Figure 2 shows the bond lengths, bond angles and bond strengths of the noncovalent bonds in these complexes calculated at the B3LYP-D3/def2-TZVPP level of theory. From NCI···NCH to NCI···$(NCH)_2$, the bond strength (binding energy) of the I···N noncovalent bond varies from 6.17 to 2.00 kcal/mol, which means that the formation of the bifurcated iodine bond weakens the I···N noncovalent bond by a surprising amount, about 68% of its magnitude. Along with this weakening, there is a large stretch of the bond length (I···N distance) by 0.357 Å, and the bond angle (∠C−I···N) becomes a lot more nonlinear. Like the case in the bifurcated hydrogen bond, it is the repulsion of two halogen bond acceptors that results in the weakening of each I···N noncovalent bond [54]. As a comparison, the formation of the pseudo-bifurcated selenium bond weakens the Se···N noncovalent bond by only about 16%. The Se···N distance is elongated by only a very small amount (0.049 Å) and the bond angle (∠C−Se···N) is decreased by only 3° upon the pseudo-bifurcated selenium bond formation. The results presented here illustrate that the two noncovalent bonds of either the true bifurcated noncovalent bond or the pseudo-bifurcated noncovalent bond reduce the strengths of each other, indicating anticooperativity. However, the anticooperative effects between two chalcogen bonds of the pseudo-bifurcated chalcogen bond are not very large as compared to those of the true bifurcated noncovalent bond. In fact, the nature of true bifurcated noncovalent bonds is that the directionality of two monocoordinate noncovalent bonds is largely destroyed. However, in the pseudo-bifurcated chalcogen bonds considered here, the directionality of two monocoordinate chalcogen bonds is kept very well, which is totally different from the true bifurcated noncovalent bonds. That is also why we use the term "pseudo-bifurcated chalcogen bond".

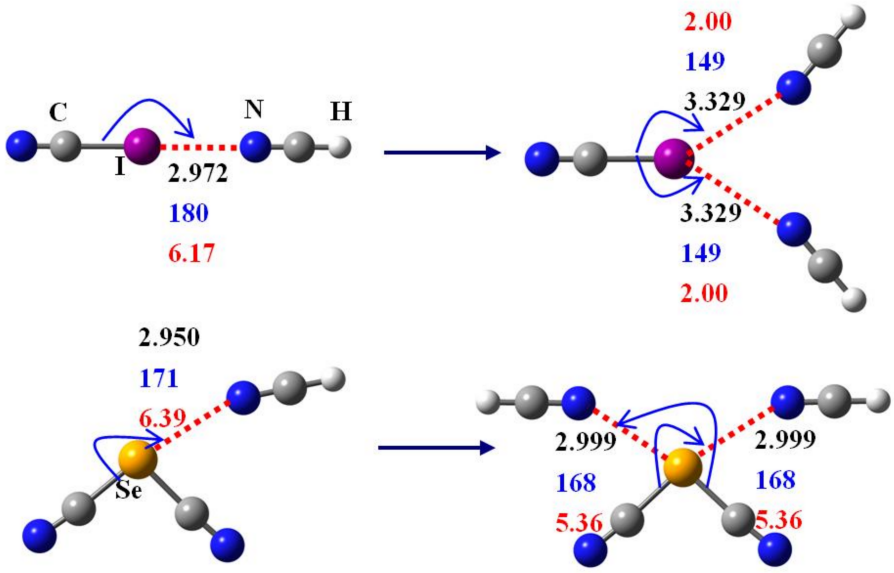

Figure 2. Bond lengths (black numbers, in Å), bond angles (blue numbers, in °) and bond strengths (red numbers, in kcal/mol) of the noncovalent bonds in the complexes NCI···NCH, NCI···$(NCH)_2$, $(NC)_2$Se···NCH and $(NC)_2$Se···$(NCH)_2$.

It is clear from Figure 2 that the strength of the pseudo-bifurcated chalcogen bond is about twice that of the "two-centered" chalcogen bond. With this in mind, we can design some strong pseudo-bifurcated chalcogen bond synthons which may have great potential in supramolecular chemistry. Figure 3 shows six complexes containing the pseudo-bifurcated chalcogen bond synthons. In these complexes, $(NC)_2$S, $(NC)_2$Se and $(NC)_2$Te are the chalcogen atom donors; Phen and TMEDA are the chalcogen atom acceptors. In a recent paper, Murray, Resnati and Politzer studied the network of $(NC)_2$Te molecules linked by many Te···N close contacts [55]. The pseudo-bifurcated chalcogen bond synthons we designed here are formed between only two molecules. As can be seen in Figure 3, the strengths of the pseudo-bifurcated chalcogen bonds are all larger than 12 kcal/mol. Therefore, the pseudo-bifurcated chalcogen bonds designed here may be used as strong synthons in crystal engineering. Chalcogen polarizability increases in the order O < S < Se < Te [56]. Thus, the strength of the pseudo-bifurcated chalcogen bond also increases in the order O < S < Se < Te. On the other hand, the sp^3 hybridized N atoms in TMEDA are much more nucleophilic than the sp^2 hybridized N atoms in Phen. Therefore, as expected, the strongest pseudo-bifurcated chalcogen bond is found in $(NC)_2$Te···TMEDA in which the binding energy is 25.34 kcal/mol. The S(Se,Te) ···N distances are also listed in Figure 3. Evidently, the strengths of the pseudo-bifurcated chalcogen bonds are inversely proportional to the S(Se,Te) ···N distances.

Both symmetric pseudo-bifurcated chalcogen bonds and asymmetrical pseudo-bifurcated chalcogen bonds have been found in the CSD. For example, the symmetric pseudo-bifurcated chalcogen bonds was found in the crystal structure of 4*H*,8*H*-4-(dicyanomethylene)benzo[1,2-*c*;4,5-*c*′]bis[1,2,5]thiadiazole (CSD entry code: GEFVOC10) [57]; the asymmetrical pseudo-bifurcated chalcogen bonds was found in the crystal structure of 4,7-difluoro-5,6-dimethoxy-2,1,3-benzoselenadiazole (CSD entry code: NABSER) [58]. The pseudo-bifurcated chalcogen bonds considered in Figure 3 are all of symmetric type. Figure 4 lists the bond lengths, bond angles and binding energies of the symmetrical pseudo-bifurcated chalcogen bond and the asymmetrical pseudo-bifurcated chalcogen bond. Obviously, the strength of the symmetrical pseudo-bifurcated chalcogen bond is almost the same as the strength of the asymmetrical pseudo-bifurcated chalcogen bond. Although similar in strength, the number of asymmetrical pseudo-bifurcated chalcogen bonds is much larger than the number of symmetrical pseudo-bifurcated chalcogen bonds because of the entropy effect.

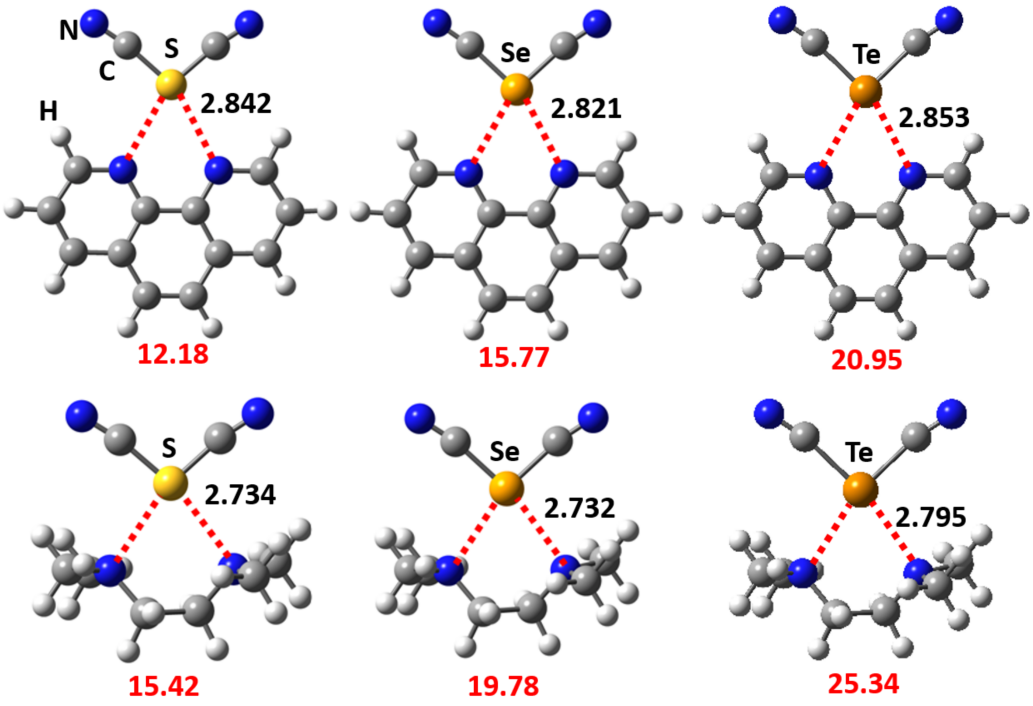

Figure 3. B3LYP-D3/def2-TZVPP binding energies (red numbers, in kcal/mol) of the complexes $(NC)_2S\cdots$Phen, $(NC)_2Se\cdots$Phen, $(NC)_2Te\cdots$Phen, $(NC)_2S\cdots$TMEDA, $(NC)_2Se\cdots$TMEDA and $(NC)_2Te\cdots$TMEDA. The chalcogen-bond lengths (in Å) are represented by black numbers.

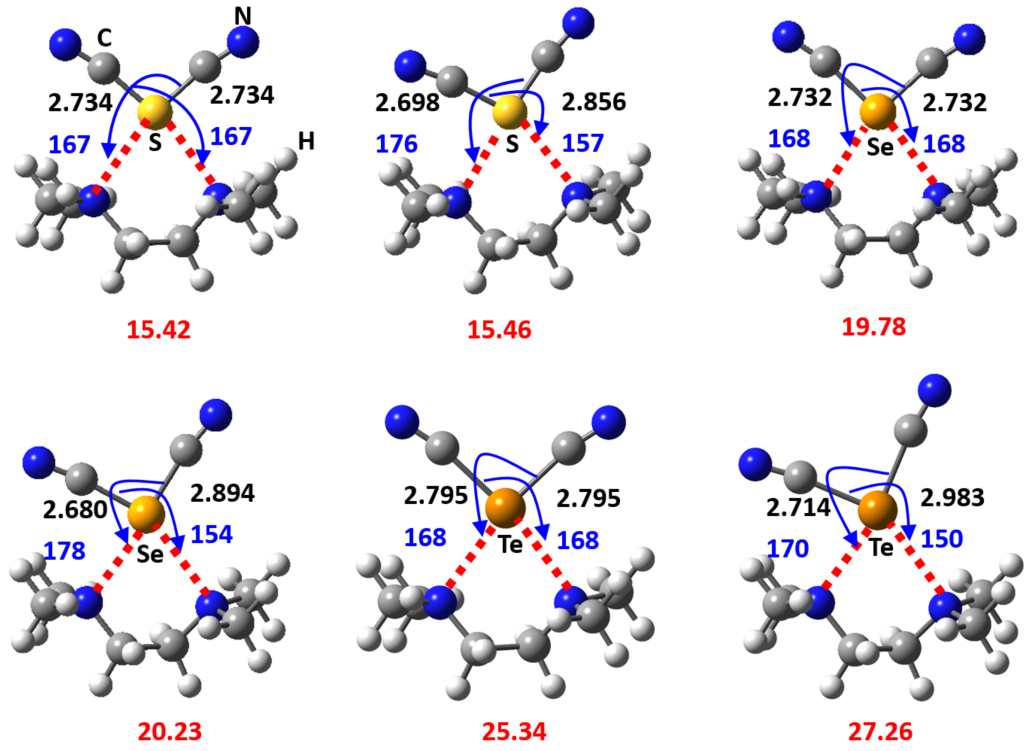

Figure 4. Bond lengths (black numbers, in Å) and bond angles (blue numbers, in °) of the symmetrical pseudo-bifurcated chalcogen bond and the asymmetrical pseudo-bifurcated chalcogen bond. The binding energies (in kcal/mol) are represented by red numbers.

Figure 5 shows the molecular graphs for the complexes $(NC)_2S\cdots$Phen, $(NC)_2Se\cdots$Phen, $(NC)_2Te\cdots$Phen, $(NC)_2S\cdots$TMEDA, $(NC)_2Se\cdots$TMEDA and $(NC)_2Te\cdots$TMEDA. The bond critical points (BCPs) of the S(Se,Te)···N contacts and the bond paths associated with the S(Se,Te)···N BCPs can be clearly seen in Figure 5. For the noncovalent bond, the electron density at the BCP is relatively low in value, and the value of the electron density Laplacian is positive [50]. As shown in Figure 5, the values of the electron density at the BCPs of the S(Se,Te)···N contacts range from 0.0198 to 0.0312 au, and the corresponding values of the electron density Laplacian range from 0.0587 to 0.0671 au. These values appear to meet the two criteria above, indicating that the S(Se,Te)···N contacts are typical noncovalent bonds. Except for the pseudo-bifurcated chalcogen bonds, there are no other noncovalent bonds in the four complexes. This is very important because it rules out the possible effects of other noncovalent bonds. The results of the AIM analyses also confirm that it is reasonable to use the binding energy of a complex as the strength of a pseudo-bifurcated chalcogen bond.

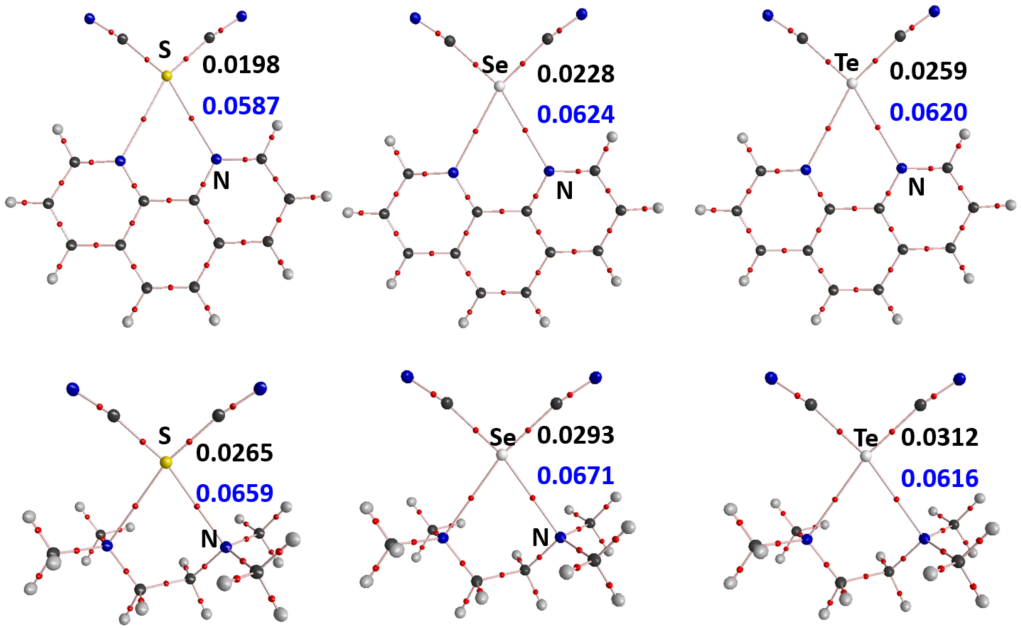

Figure 5. Molecular graphs for the complexes $(NC)_2S\cdots$Phen, $(NC)_2Se\cdots$Phen, $(NC)_2Te\cdots$Phen, $(NC)_2S\cdots$TMEDA, $(NC)_2Se\cdots$TMEDA and $(NC)_2Te\cdots$TMEDA. Small red dots represent the bond critical points and ring critical points are omitted for clarity. The values of the electron density (au) and its Laplacian (au) at the S(Se,Te)–N bond critical points are represented by the black numbers and blue numbers, respectively.

4. Conclusions

In the present study, we have proposed a new kind of noncovalent bond—pseudo-bifurcated chalcogen bond—since the chalcogens may have two electrophilic σ holes. The difference between the pseudo-bifurcated noncovalent bonds and the true bifurcated noncovalent bonds was investigated by using the dispersion-corrected density functional theory calculations. It was found that the anticooperative effects between two chalcogen bonds of the pseudo-bifurcated chalcogen bond are not very large comparing with those of the true bifurcated noncovalent bond. According to the nature of pseudo-bifurcated chalcogen bond, we designed a series of strong pseudo-bifurcated chalcogen bond synthons of which the strengths are all larger than 12 kcal/mol. We wish these strong pseudo-bifurcated chalcogen bond synthons to have great potential in crystal engineering.

Acknowledgments: This work was supported by the National Science Foundation of China (21773104) and the Program for Science & Technology Innovation Talents in Universities of Henan Province (13HASTIT015). Computer time was provided by National Supercomputing Center in Shenzhen.

Author Contributions: Yu Zhang performed the CSD search and analyzed the data. Yu Zhang carried out the quantum chemical calculations. Weizhou Wang supervised the research. All authors made equal contributions in writing of manuscript.

Conflicts of Interest: The authors declare no conflict of interest.

References

1. Metrangolo, P.; Meyer, F.; Pilati, T.; Resnati, G.; Terraneo, G. Halogen Bonding in Supramolecular Chemistry. *Angew. Chem. Int. Ed.* **2008**, *47*, 6114–6127. [CrossRef] [PubMed]
2. Bertani, R.; Sgarbossa, P.; Venzo, A.; Lelj, F.; Amati, M.; Resnati, G.; Pilati, T.; Metrangolo, P.; Terraneo, G. Halogen Bonding in Metal–Organic–Supramolecular Networks. *Coord. Chem. Rev.* **2010**, *254*, 677–695. [CrossRef]
3. Cavallo, G.; Metrangolo, P.; Pilati, T.; Resnati, G.; Sansotera, M.; Terraneo, G. Halogen Bonding: A General Route in Anion Recognition and Coordination. *Chem. Soc. Rev.* **2010**, *39*, 3772–3783. [CrossRef] [PubMed]
4. Riley, K.E.; Hobza, P. Investigations into the Nature of Halogen Bonding Including Symmetry Adapted Perturbation Theory Analyses. *J. Chem. Theory Comput.* **2008**, *4*, 232–242. [CrossRef] [PubMed]
5. Pennington, W.T.; Resnati, G.; Taylor, M.S. Halogen Bonding: From Self-Assembly to Materials and Biomolecules. *CrystEngComm* **2013**, *15*, 3057. [CrossRef]
6. Desiraju, G.R.; Ho, P.S.; Kloo, L.; Legon, A.C.; Marquardt, R.; Metrangolo, P.; Politzer, P.; Resnati, G.; Rissanen, K. Definition of the Halogen Bond. *Pure Appl. Chem.* **2013**, *85*, 1711–1713. [CrossRef]
7. Cavallo, G.; Metrangolo, P.; Pilati, T.; Resnati, G.; Terraneo, G. Naming Interactions from the Electrophilic Site. *Cryst. Growth Des.* **2014**, *14*, 2697–2702. [CrossRef]
8. Giese, M.; Albrecht, M.; Rissanen, K. Anion−π Interactions with Fluoroarenes. *Chem. Rev.* **2015**, *115*, 8867–8895. [CrossRef] [PubMed]
9. Gilday, L.C.; Robinson, S.W.; Barendt, T.A.; Langton, M.J.; Mullaney, B.R.; Beer, P.D. Halogen Bonding in Supramolecular Chemistry. *Chem. Rev.* **2015**, *115*, 7118–7195. [CrossRef] [PubMed]
10. Cavallo, G.; Metrangolo, P.; Milani, R.; Pilati, T.; Priimagi, A.; Resnati, G.; Terraneo, G. The Halogen Bond. *Chem. Rev.* **2016**, *116*, 2478–2601. [CrossRef] [PubMed]
11. Wang, H.; Wang, W.; Jin, W.J. σ-Hole Bond vs. π-Hole Bond: A Comparison Based on Halogen Bond. *Chem. Rev.* **2016**, *116*, 5072–5104. [CrossRef] [PubMed]
12. Kolář, M.H.; Hobza, P. Computer Modeling of Halogen Bonds and Other σ-Hole Interactions. *Chem. Rev.* **2016**, *116*, 5155–5187. [CrossRef] [PubMed]
13. Kapecki, J.A.; Baldwin, J.E. Extended Hueckel Calculations on Two Heterocyclic Systems Containing 2.41- and 2.64-Å Sulfur-Oxygen Distances. *J. Am. Chem. Soc.* **1969**, *91*, 1120–1123. [CrossRef]
14. Rosenfield, R.E., Jr.; Parthasarathy, R.; Dunitz, J.D. Directional Preferences of Nonbonded Atomic Contacts with Divalent Sulfur. 1. Electrophiles and Nucleophiles. *J. Am. Chem. Soc.* **1977**, *99*, 4860–4862. [CrossRef]
15. Guru Row, T.N.; Parthasarathy, R. Directional Preferences of Nonbonded Atomic Contacts with Divalent Sulfur in Terms of its Orbital Orientations. 2. Sulfur···Sulfur Interactions and Nonspherical Shape of Sulfur in Crystals. *J. Am. Chem. Soc.* **1981**, *103*, 477–479.
16. Iwaoka, M.; Takemoto, S.; Tomoda, S. Statistical and Theoretical Investigations on the Directionality of Nonbonded S···O Interactions. Implications for Molecular Design and Protein Engineering. *J. Am. Chem. Soc.* **2002**, *124*, 10613–10620. [CrossRef] [PubMed]
17. Werz, D.B.; Gleiter, R.; Rominger, F. Nanotube Formation Favored by Chalcogen−Chalcogen Interactions. *J. Am. Chem. Soc.* **2002**, *124*, 10638–10639. [CrossRef] [PubMed]
18. Cozzolino, A.F.; Vargas-Baca, I.; Mansour, S.; Mahmoudkhani, A.H. The Nature of the Supramolecular Association of 1,2,5-Chalcogenadiazoles. *J. Am. Chem. Soc.* **2005**, *127*, 3184–3190. [CrossRef] [PubMed]
19. Bleiholder, C.; Werz, D.B.; Köppel, H.; Gleiter, R. Theoretical Investigations on Chalcogen−Chalcogen Interactions: What Makes These Nonbonded Interactions Bonding? *J. Am. Chem. Soc.* **2006**, *128*, 2666–2674. [CrossRef] [PubMed]
20. Bleiholder, C.; Gleiter, R.; Werz, D.B.; Köppel, H. Theoretical Investigations on Heteronuclear Chalcogen−Chalcogen Interactions: On the Nature of Weak Bonds between Chalcogen Centers. *Inorg. Chem.* **2007**, *46*, 2249–2260. [CrossRef] [PubMed]

21. Wang, W.; Ji, B.; Zhang, Y. Chalcogen Bond: A Sister Noncovalent Bond to Halogen Bond. *J. Phys. Chem. A* **2009**, *113*, 8132–8135. [CrossRef] [PubMed]
22. Manna, D.; Mugesh, G. Regioselective Deiodination of Thyroxine by Iodothyronine Deiodinase Mimics: An Unusual Mechanistic Pathway Involving Cooperative Chalcogen and Halogen Bonding. *J. Am. Chem. Soc.* **2012**, *134*, 4269–4279. [CrossRef] [PubMed]
23. Metrangolo, P.; Resnati, G. Enzyme Mimics: Halogen and Chalcogen Team up. *Nat. Chem.* **2012**, *4*, 437–438. [CrossRef] [PubMed]
24. Li, Q.Z.; Li, R.; Guo, P.; Li, H.; Li, W.Z.; Cheng, J.B. Competition of Chalcogen Bond, Halogen Bond, and Hydrogen Bond in SCS–HOX and SeCSe–HOX (X = Cl and Br) Complexes. *Comput. Theor. Chem.* **2012**, *980*, 56–61. [CrossRef]
25. Bauzá, A.; Quiñonero, D.; Deyà, P.M.; Frontera, A. Halogen Bonding versus Chalcogen and Pnicogen Bonding: A Combined Cambridge Structural Database and Theoretical Study. *CrystEngComm* **2013**, *15*, 3137–3144. [CrossRef]
26. Scheiner, S. The Pnicogen Bond: Its Relation to Hydrogen, Halogen, and Other Noncovalent Bonds. *Acc. Chem. Res.* **2013**, *46*, 280–288. [CrossRef] [PubMed]
27. Azofra, L.M.; Scheiner, S. Substituent Effects in the Noncovalent Bonding of SO_2 to Molecules Containing a Carbonyl Group. The Dominating Role of the Chalcogen Bond. *J. Phys. Chem. A* **2014**, *118*, 3835–3845. [CrossRef] [PubMed]
28. Bai, M.; Thomas, S.P.; Kottokkaran, R.; Nayak, S.K.; Ramamurthy, P.C.; Guru Row, T.N. A Donor–Acceptor–Donor Structured Organic Conductor with S···S Chalcogen Bonding. *Cryst. Growth Des.* **2014**, *14*, 459–466. [CrossRef]
29. Fanfrlík, J.; Přáda, A.; Padělková, Z.; Pecina, A.; Macháček, J.; Lepšík, M.; Holub, J.; Růžička, A.; Hnyk, D.; Hobza, P. The Dominant Role of Chalcogen Bonding in the Crystal Packing of 2D/3D Aromatics. *Angew. Chem. Int. Ed.* **2014**, *53*, 10139–10142. [CrossRef] [PubMed]
30. Benz, S.; López-Andarias, J.; Mareda, J.; Sakai, N.; Matile, S. Catalysis with Chalcogen Bonds. *Angew. Chem. Int. Ed.* **2017**, *56*, 812–815. [CrossRef] [PubMed]
31. Geboes, Y.; De Vleeschouwer, F.; De Proft, F.; Herrebout, W.A. Exploiting the σ-Hole Concept: An Infrared and Raman-Based Characterization of the S···O Chalcogen Bond between 2,2,4,4-Tetrafluoro-1,3-dithiethane and Dimethyl Ether. *Chem. Eur. J.* **2017**, *23*, 17384–17392. [CrossRef] [PubMed]
32. Mahmudov, K.T.; Kopylovich, M.N.; Guedes da Silva, M.F.C.; Pombeiro, A.J.L. Chalcogen Bonding in Synthesis, Catalysis and Design of Materials. *Dalton Trans.* **2017**, *46*, 10121–10138. [CrossRef] [PubMed]
33. Brammer, L. Halogen Bonding, Chalcogen Bonding, Pnictogen Bonding, Tetrel Bonding: Origins, Current Status and Discussion. *Faraday Discuss.* **2017**, *203*, 485–507. [CrossRef] [PubMed]
34. Legon, A.C. Tetrel, Pnictogen and Chalcogen Bonds Identified in the Gas Phase before They Had Names: A Systematic Look at Non-Covalent Interactions. *Phys. Chem. Chem. Phys.* **2017**, *19*, 14884–14896. [CrossRef] [PubMed]
35. Guseinov, F.I.; Pistsov, M.F.; Movsumzade, E.M.; Kustov, L.M.; Tafeenko, V.A.; Chernyshev, V.V.; Gurbanov, A.V.; Mahmudov, K.T.; Pombeiro, A.J.L. Tetrel, Chalcogen, and Charge-Assisted Hydrogen Bonds in 2-((2-Carboxy-1-(substituted)-2-hydroxyethyl)thio) Pyridin-1-ium Chlorides. *Crystals* **2017**, *7*, 327. [CrossRef]
36. Mikherdov, A.S.; Novikov, A.S.; Kinzhalov, M.A.; Zolotarev, A.A.; Boyarskiy, V.P. Intra-/Intermolecular Bifurcated Chalcogen Bonding in Crystal Structure of Thiazole/Thiadiazole Derived Binuclear (Diaminocarbene)Pd^{II} Complexes. *Crystals* **2018**, *8*, 112. [CrossRef]
37. Sedlak, R.; Eyrilmez, S.M.; Hobza, P.; Nachtigallova, D. The Role of the σ-Holes in Stability of Non-Bonded Chalcogenide···Benzene Interactions: The Ground and Excited States. *Phys. Chem. Chem. Phys.* **2018**, *20*, 299–306. [CrossRef] [PubMed]
38. Wang, H.; Liu, J.; Wang, W. Intermolecular and Very Strong Intramolecular C–Se···O/N Chalcogen Bonds in Nitrophenyl Selenocyanate Crystals. *Phys. Chem. Chem. Phys.* **2018**, *20*, 5227–5234. [CrossRef] [PubMed]
39. Clark, T.; Hennemann, M.; Murray, J.S.; Politzer, P. Halogen Bonding: The *σ*-Hole. *J. Mol. Model.* **2007**, *13*, 291–296. [CrossRef] [PubMed]
40. Murray, J.S.; Lane, P.; Clark, T.; Politzer, P. *σ*-Hole Bonding: Molecules Containing Group VI Atoms. *J. Mol. Model.* **2007**, *13*, 1033–1038. [CrossRef] [PubMed]

41. Murray, J.S.; Lane, P.; Clark, T.; Riley, K.E.; Politzer, P. σ-Holes, π-Holes and Electrostatically-Driven Interactions. *J. Mol. Model.* **2012**, *18*, 541–548. [CrossRef] [PubMed]
42. Politzer, P.; Murray, J.S.; Clark, T. Halogen Bonding: An Electrostatically-Driven Highly Directional Noncovalent Interaction. *Phys. Chem. Chem. Phys.* **2010**, *12*, 7748–7757. [CrossRef] [PubMed]
43. Allen, F.H. The Cambridge Structural Database: A Quarter of a Million Crystal Structures and Rising. *Acta Crystallogr. Sect. B* **2002**, *58*, 380–388. [CrossRef]
44. Allen, F.H.; Motherwell, W.D.S. Applications of the Cambridge Structural Database in Organic Chemistry and Crystal Chemistry. *Acta Crystallogr. Sect. B* **2002**, *58*, 407–422. [CrossRef]
45. Grimme, S.; Antony, J.; Ehrlich, S.; Krieg, H. A Consistent and Accurate *Ab Initio* Parametrization of Density Functional Dispersion Correction (DFT-D) for the 94 Elements H-Pu. *J. Chem. Phys.* **2010**, *132*, 154104. [CrossRef] [PubMed]
46. Weigend, F.; Ahlrichs, R. Balanced Basis Sets of Split Valence, Triple Zeta Valence and Quadruple Zeta Valence Quality for H to Rn: Design and Assessment of Accuracy. *Phys. Chem. Chem. Phys.* **2005**, *7*, 3297–3305. [CrossRef] [PubMed]
47. Grimme, S.; Ehrlich, S.; Goerigk, L. Effect of the Damping Function in Dispersion Corrected Density Functional Theory. *J. Comput. Chem.* **2011**, *32*, 1456–1465. [CrossRef] [PubMed]
48. Boys, S.F.; Bernardi, F. The Calculation of Small Molecular Interactions by the Difference of Separate Total Energies. Some Procedures with Reduced Errors. *Mol. Phys.* **1970**, *19*, 553–566. [CrossRef]
49. Frisch, M.J.; Trucks, G.W.; Schlegel, H.B.; Scuseria, G.E.; Robb, M.A.; Cheeseman, J.R.; Scalmani, G.; Barone, V.; Mennucci, B.; Petersson, G.A.; et al. *Gaussian 09, Revision C.01*; Gaussian, Inc.: Wallingford, CT, USA, 2010.
50. Bader, R.F.W. *Atoms in Molecules—A Quantum Theory*; Oxford University Press: Oxford, UK, 1990.
51. Popelier, P.L.A. Characterization of a Dihydrogen Bond on the Basis of the Electron Density. *J. Phys. Chem. A* **1998**, *102*, 1873–1878. [CrossRef]
52. Wang, W.; Wong, N.B.; Zheng, W.; Tian, A. Theoretical Study on the Blueshifting Halogen Bond. *J. Phys. Chem. A* **2004**, *108*, 1799–1805. [CrossRef]
53. Biegler-König, F.; Schönbohm, J.; Bayles, D. AIM2000-A Program to Analyze and Visualize Atoms in Molecules. *J. Comput. Chem.* **2001**, *22*, 545–559.
54. Steiner, T. The Hydrogen Bond in the Solid State. *Angew. Chem. Int. Ed.* **2002**, *41*, 48–76. [CrossRef]
55. Murray, J.S.; Resnati, G.; Politzer, P. Close Contacts and Noncovalent Interactions in Crystals. *Faraday Discuss.* **2017**, *203*, 113–130. [CrossRef] [PubMed]
56. Lide, D.R. (Ed.) *Handbook of Chemistry and Physics*, 87th ed.; CRC: Boca Raton, FL, USA, 2006.
57. Suzuki, T.; Fujii, H.; Yamashita, Y.; Kabuto, C.; Tanaka, S.; Harasawa, M.; Mukai, T.; Miyashi, T. Clathrate Formation and Molecular Recognition by Novel Chalcogen-Cyano Interactions in Tetracyanoquinodimethanes Fused with Thiadiazole and Selenadiazole Rings. *J. Am. Chem. Soc.* **1992**, *11*, 3034–3043. [CrossRef]
58. Mikhailovskaya, T.F.; Makarov, A.G.; Selikhova, N.Y.; Makarov, A.Y.; Pritchina, E.A.; Bagryanskaya, I.Y.; Vorontsova, E.V.; Ivanov, I.D.; Tikhova, V.D.; Gritsan, N.P.; et al. Carbocyclic Functionalization of Quinoxalines, Their Chalcogen Congeners 2,1,3-Benzothia/Selenadiazoles, and Related 1,2-Diaminobenzenes Based on Nucleophilic Substitution of Fluorine. *J. Fluorine Chem.* **2016**, *183*, 44–58. [CrossRef]